

## Modelling of CO<sub>2</sub> Sequestration in Deep Saline Aquifer Reservoir Using Surface Evolver Software

Pradeep Kumar

Bhabha Atomic Research Centre, Trombay, Mumbai, India, 400085.

E-mail: [pradeepk@barc.gov.in](mailto:pradeepk@barc.gov.in)

Received: 10.12.2023, Revised: 29.1.2024, 30.1.2024, Accepted: 30.1.2024

### Abstract

A strategy to mitigate CO<sub>2</sub> concentration in the atmosphere is injection of supercritical CO<sub>2</sub> in porous sedimentary medium filled with saline water where CO<sub>2</sub> gets trapped in the pores. Sequestration is resultant of two processes, drainage and imbibition in accordance with capillary law. Simulation of the pore-scale trapping has been performed on reservoir scale. A simple model reservoir consisting of 1000 tetrahedral subunits was constructed. Using Surface Evolver software, pore volume of each tetrahedral subunit and liquid saturation in the model reservoir were calculated. Normalized critical curvature for drainage and imbibition were evaluated for each subunit. The CO<sub>2</sub> pressure and liquid saturation curves of the reservoir displayed hysteretic character, indicating that the evolution of the system is pathway-dependent. The simulated curves illustrate the pathway dependency of the residual gas saturation, an important parameter controlling the amount of CO<sub>2</sub> stored in the reservoir, hence the efficiency of the CO<sub>2</sub> storage. Our study also shows the existence of critical thresholds in terms of in/out gassing during the drainage or imbibition processes.

**Key Words** Reservoir, Drainage, Imbibition, Hysteresis

### Introduction

In the previous article<sup>1</sup> published in this journal, pore scale investigation of CO<sub>2</sub> sequestration in sedimentary media has been described. The medium modelled as random packing of equal spheres, giving rise to a network of pore bodies connected by pore throats. The basic laws of capillarity are integrated to understand the CO<sub>2</sub> gas trapping processes at the pore scale. The two key processes, drainage and imbibition, responsible for CO<sub>2</sub> sequestration have been studied using the Surface Evolver software<sup>2</sup>. Starting from liquid bridge adhering between two spheres, subsequently extended to liquid bridge adhering to three spheres and drainage and imbibition in pore throat have been investigated.

In the present paper, study has been extended to CO<sub>2</sub> trapping at reservoir scale. Reservoir is modelled as 3D network of large number of pore bodies connected by pore throats. The

pore is described in terms of tetrahedral subunits, centers of four spheres lying on the vertices of a tetrahedron. The void space inside the tetrahedron has been termed as pore body while the cross section of each face as pore throat. Initially drainage and imbibition processes are modelled at pore body for regular polyhedron. For reservoir, the heterogeneity is taken into consideration by means of distance variation among spheres.

### **Experimental**

In the beginning, the entire reservoir contained the resident saline solution completely saturating the pores constituting a continuous wetting phase. During the drainage process, the non-wetting phase ( $\text{CO}_2$ ) displaces the wetting phase (liquid) from the pores and progressively invades the pores network. At the extreme, the  $\text{CO}_2$  forms a continuously connecting air bubble throughout the entire reservoir (pore network), and the residual water only persisting as pendular rings. The drainage process involves the receding of the meniscus ( $\text{CO}_2$ -brine interface) into the pore body, successively partitioning into several individual liquid bridges. The process occurs under the influence of two key parameters: the capillary pressure and the local geometry. In the present study simulations have been performed for various processes such as simulation of pore body drainage, simulation of pore body imbibition, imbibition at the pore throat. Simulation of drainage and imbibition for model reservoir has been performed.

#### **(a) Simulation of Pore Body Drainage**

At the pore scale simulation, liquid bridge adheres to four spheres arranged in a tetrahedral configuration. The arrival of the gas bubble is important event. This means building of a liquid-gas interface, which can pass through a pore body. Hence, the capillary properties of the pores determine the drainage of the pore bodies. Owing to tetrahedral configuration of pore, the interface can enter the pore from any of the four faces (pore throat) formed by three triangle-arranged spheres. In other words, the most critical step during a drainage process, is the conditions and situation where the pore body is emptied while the wedge-shaped parts remain filled.

The capillary pressure is a direct function of the curvature of the interface. The curvature gradually increases with the pressure. During injection period, the gas pressure increases significantly whereas variation in the liquid pressure is negligible. During injection period, a certain state is reached where interface passes into the pore body: the liquid spontaneously drains from the pore body and bubble goes on moving towards another network subunit. This spontaneous invasion is often termed as the Haines jump<sup>3</sup> and the corresponding curvature is

called the critical curvature. The Mayer-Stowe-Princeton (MS-P) method<sup>4</sup> is an accurate analytical method for calculating the critical curvature of complex geometries and yields satisfactory results for meniscus in pores formed by rods. Mason and Marrow<sup>5,6</sup> experimentally observed that the MS-P theory provides good approximation to meniscus in pore throats formed by spheres as well, and so the curvatures were calculated using this MS-P method.

Following the simulation (Fig. 2), small CO<sub>2</sub> volume is held in pore throats before reaching the critical curvature, and it gradually increases with capillary pressure while the corresponding liquid volume is displaced. At the critical curvature conditions, CO<sub>2</sub> invades the pore body forcing the liquid out from the pore body. As a consequence, the CO<sub>2</sub> is percolating throughout the given subunit, while the water remains as pendular rings. Further increase in capillary conditions does not significantly enhance the CO<sub>2</sub> trapping. The liquid water in pendular rings corresponds to residual water saturation.

#### **(b) Simulation of Imbibition**

The imbibition process is the reverse of drainage process: pores are invaded by the wetting phase. Imbibition leads to formation of continuous liquid phase, implying the splitting of the CO<sub>2</sub> bubble into dispersed air pockets inside the porous medium. The imbibition process starts from the point where the drainage has ended. Here also, the location and shape of the interface is described by the capillary pressure, and the geometry of the portion of the pore hosting the interface. The imbibition is simulated through the incremental decrease in the capillary pressure gradually allowing water to invade the sampling network, thereby increasing the water saturation in the system. Thus, as the imbibition progresses, the capillary pressure correspondingly decreases, and the related configuration and location of the interface change. The interface moves reversibly in response to this decrement in the capillary pressure, as long as another interface is not encountered. Irreversible pore-level imbibition event occurs when decrement in pressure causes two interfaces to touch with each other, spontaneously merging into single interface. Now, restoring the pressure to prior values would not cause the wetting phase to split into its pre-merger situation: this fact is the true basis of what is classically called the hysteresis, namely the fact that the drying and the wetting branches do not correspond in terms of pressure-volume relationship. Clearly, the imbibition process disconnects the earlier continuous CO<sub>2</sub> phase.

**(c) Imbibition at the Pore Throat**

The imbibition process starts from the end point of the primary drainage (irreducible water saturation or any turning point of interest), and the capillary existing inside three pendular rings progressively decreases. As a consequence, the rings start growing and finally merge so that the entire plane delimited by three spheres is filled with liquid: CO<sub>2</sub> is spontaneously eliminated from this portion of the throat, disconnecting the gas phase. This type of imbibition is called coalescence or snap-off, and its main characteristic is that it preserves the hosted CO<sub>2</sub> bubble at the very centre of a tetrahedral sub-unit. Thus the continuous CO<sub>2</sub> phase becomes discontinuous, with the very positive feed-back (in terms of storage efficiency) of trapping air pockets surrounded by liquid barriers. The isolated CO<sub>2</sub> bubble, present in the pore body of the tetrahedral sub unit, is trapped under stable conditions (as long as the conditions do not change).

**(d) Imbibition at the Pore Body**

After the throat imbibition, a liquid bridge exists adhering to three spheres while the pore body entrance hosts the brine-CO<sub>2</sub> meniscus. On further decreasing the capillary pressure, the liquid bridge as well as the meniscus would grow in size, finally merging with each other. Such merging leads to spontaneous withdrawal of CO<sub>2</sub> phase from the pore body, or conversely leading to the spontaneous filling-up of the pore. Haines<sup>3</sup> proposed an approximation to evaluate the critical curvature of imbibition. The meniscus in the pore is approximated to a sphere that just touches four spheres (nil contact angle). The imbibition curvature ( $C_{imb}$ ) is therefore expressed by the following relation.

$$C_{imb} = \frac{2R}{r_{cav}} \quad (1)$$

Where 'R' is the radius of sphere and 'r<sub>cav</sub>' is the radius of the in-sphere space. However, the drainage critical curvature calculated by MS-P method and the imbibition critical curvature calculated by Haines in-sphere approximation, resulted in a negative hysteresis, known to be practically impossible. As a consequence, Mason and Mellor<sup>7</sup> suggested on sound grounds an empirical shift to the Haines values in order to eliminate the hysteric effect. Accordingly, they suggested the following relationship:

$$C_{imb} = \frac{2R}{r_{cav}} - 1.6 \quad (2)$$

Using these formulae, the pressure-volume relationships were derived along the different steps

described in Fig. 3. Obviously, the imbibition at the pore throat occurs at higher pressure than the imbibition at the pore body. Initially, only one of the throats gets imbided, and after a certain range of capillarization inside the system, the pore body itself gets imbided (Fig. 3). Along the imbibition pathway, it becomes evident that much larger CO<sub>2</sub> amount gets trapped than along the drainage pathway.

**(e) Simulation of drainage and imbibition for model reservoir and hysteresis in capillary pressure**

So far, we have carried out pore scale investigation for single regular tetrahedron. These investigations have provided direct insight on the role of the geometry on the drainage and imbibition processes at the pore level. At the reservoir scale, the sequestration is expressed by capillary pressure versus the liquid saturation graph, and so the principle of the simulation and the lines of interpretation remain similar.

However, while carrying out simulation for a large scale reservoir, it is imperative to take into consideration the degree of heterogeneity, at least defining a certain range of existing porosity. In the pore level approach, the reservoir is modelled as random packing of equal spheres while at the basin scale, integration of grain size variation is required. To make preliminary estimation, we have built a model reservoir consisting of a network of irregular tetrahedrons, by using equal-size spheres separated by varying distances. As a consequence, the hosting porosity is changing throughout the media in a way analogous to what occurred in nature with varying grain size.

Actually, the distance between the centres of two spheres constitutes the edge of the tetrahedron. For a reservoir consisting of random packing of equal spheres, most often the spheres are in contact with each other. Meanwhile, for separated spheres, all edge lengths of tetrahedron are almost equally probable up to 1.4 times the sphere diameter<sup>7</sup>. In the tetrahedral subunits, one sphere was assumed to be in contact with the other three spheres, whereas for separated spheres all possible combinations of edge lengths (again, up to 1.4 times the sphere diameter) were taken into consideration for the construction of irregular tetrahedral subunits. A simple model reservoir was constructed consisting of 1000 tetrahedral subunits. Pore volume for each subunit was calculated and liquid saturation in the model reservoir was obtained. Similarly, normalized critical curvature for drainage and imbibition were calculated for each subunit. The imbibition critical curvatures are lesser than the

drainage critical curvatures (Fig. 4, on only 200 pores statistically chosen), according to the above described processes.

To drain a subunit, the gas-liquid interface would enter from the face (throat) having the smallest capillary pressure, i.e. the smallest drainage critical curvature. The critical curvature obviously decreases with the widening of the distance between the spheres. Hence, it is easier to penetrate the pore body through the face having large distance between the spheres (smallest capillary pressure between the three faces). The respective amount of liquid and trapped CO<sub>2</sub> depends upon the pore volume itself as per the edge lengths constituting the tetrahedral subunit. Two pores can possess the same volume even with different combination of edge lengths. With widening the distance between spheres, the pore volume increases while the interface curvature decreases: larger pores are easier to drain. Initially the model reservoir is assumed to be completely filled with liquid phase (100% liquid saturation). For the model reservoir, the drainage process was simulated by successively draining the pores in the order of their increasing drainage critical curvature and calculating the corresponding liquid/CO<sub>2</sub> saturation in the reservoir as well as capillary pressure (Fig- 5). The model reservoir shows ~7% residual water saturation, a value calculated as the remaining liquid amount (trapped as pendular rings) when the drainage emptied even the smallest pore throats/bodies of the model reservoir.

After having reached the residual liquid water saturation, the simulation makes the capillary pressure to progressively decrease. As a consequence, the pores of the model reservoir get imbibed following the order of the decreasing imbibition critical curvature. As mentioned earlier, the liquid/CO<sub>2</sub> saturation and the capillary pressure can be calculated along the imbibition. Owing to the tetrahedral structure of pore body, the critical drainage curvature and imbibitions curvature are different: imbibition occurs at lower curvature than drainage, this leads to hysteric effect<sup>8</sup>. In other words, drainage depends on the critical curvature of the pore throat whereas the imbibition depends upon the pore body. As a consequence, the imbibition curves plot at lower pressure than the drainage curve (Fig-5), and such curves are often called hysteretic curves. During the imbibition process, CO<sub>2</sub> gets trapped in some pores depending upon the injection conditions of the reservoir, e.g. the capillary number. Suekane et al.<sup>7</sup> have experimentally observed the presence of a residual gas saturation (after the final stage of imbibition) and found it to depend on the capillary number, namely the ratio between the velocity of the liquid-gas interface and the interfacial tension. For low capillary numbers, flow in porous media is dominated by capillary forces. Very logically, Suekane et al.<sup>7</sup> concluded that the residual gas saturation decreases as the capillary number increases.

We decided to calculate the value of this residual gas saturation by fixing arbitrarily the percentage of pores keeping its gas bubbles in the final stage of the process. We have chosen three situations: 10%, 20%, 30% of pores trapped by CO<sub>2</sub>, resulting in residual gas saturations of 10%, 17% and 26%, respectively (Fig. 5).

Another important parameter that needs to be considered is the saturation existing at the state where the system changes from drainage to imbibition, called the turning point (Fig. 6). According to the concepts developed above, at any turning point above the irreducible liquid saturation, some pores contain large amount of CO<sub>2</sub> along with liquid pendular rings and are ready to the imbibition stage, while others are still almost entirely filled with liquid. As a consequence, when turning to the imbibition stage, the first type of pores can trap CO<sub>2</sub> bubbles and contribute to the residual gas saturation while the latter do not experience significant changes. For a given model reservoir, certain percentage of pores participate in the residual gas saturation, then the irreducible gas saturation depends mainly upon the saturation value at the turning point (Fig. 6).

The higher the reservoir is liquid saturated at the turning point (the lesser is the number of pores experiencing the complete emptying), the lesser is the residual gas saturation (Fig. 6). The maximum residual gas saturation corresponds to the turning point at the irreducible liquid saturation.

## **Results and Discussion**

In the present study, starting from simulation of drainage and imbibition processes of tetrahedral subunits, was extended to reservoir scale. The reservoir was modelled as random packing of equal spheres consisting of 1000 tetrahedral subunits giving rise to 3-D network of pore bodies and pore throats. The heterogeneity aspect of reservoir was taken into consideration by varying the distance between two equal-size spheres upto 1.4 times the side length. The drainage and imbibition processes are governed by the capillary pressure and the local geometry. For a tetrahedral subunit, pore body drainage was simulated in terms of as progressively increasing curvature of gas-liquid (CO<sub>2</sub>-brine) interface. The interface penetrates through face formed by triangle configuration of spheres .

During the CO<sub>2</sub> injection period, at certain point interface passes into the pore body and the liquid spontaneously drains from the pore body, gas bubble goes on moving towards another network subunit. Critical curvature was calculated by Mayer-Stowe-Princeton (MS-P) method. Imbibition causes the splitting of the CO<sub>2</sub> bubble into dispersed air pockets inside

the porous medium. Irreversible pore-level imbibition takes place when two interfaces touch with each other, spontaneously merging into single interface. Imbibition occur at throat where the pendular rings start growing and finally merge, CO<sub>2</sub> is spontaneously eliminated from this portion of the throat, disconnecting the gas phase. This type of imbibition is called coalescence or snap-off. On further decreasing the capillary pressure, the liquid bridge as well as the meniscus inside pore body would grow in size, finally merging with each other, leading to spontaneous withdrawal of CO<sub>2</sub> phase from the pore body, or conversely leading to the spontaneous filling-up of the pore. Haines approximation, modified by Mason and Mellor was employed to evaluate the critical curvature of imbibition.

On similar lines, simulation for reservoir was carried out. At the reservoir scale, the sequestration is expressed by capillary pressure versus the liquid saturation graph. Using Surface Evolver software, pore volume for each subunit and liquid saturation in the model reservoir was obtained. Also Normalized critical curvature for drainage and imbibition were calculated for each subunit. The imbibition critical curvatures are lesser than the drainage critical curvatures. The drainage occurs during CO<sub>2</sub> injection in the system whereas imbibition occurs during post injection period. The study revealed that the system is highly pathway-dependent, indicating hysteretic character of the pressure-volume curves. This can be assigned to the fact that the imbibition curvature is lesser than drainage curvature. The gas trapping in reservoirs as gas bubbles gets stabilized inside the pore bodies or pore throats, may be very efficient and could be expected to be a major parameter in the gas storage amount.

On the CO<sub>2</sub> sequestration point of view, the residual gas saturation is of the utmost importance, since it determine the amount of CO<sub>2</sub> permanently trapped as gas bubbles, a parameter that directly participates in the efficiency of the global storage operation. One major features outlined by our study is the strong dependency of this residual gas saturation, on the pathway followed by the bubble during the post-injection period. The more the bubble disperses throughout the media, the more drained is the reservoir, the more CO<sub>2</sub> will be finally trapped. On the contrary, whenever the injected massive bubble slides inside the reservoir without splitting in many interfaces throughout the pores, the less drained is the reservoir implying that the final gas trapping is drastically reduced.

## **Conclusions**

In the present study we have performed modelling of CO<sub>2</sub> sequestration in deep saline aquifers using surface evolver software. The actual reservoir is very complex. For sake of



simplicity, the reservoir is modelled as random packing of equal spheres which nearly mimicks real reservoir. Drainage and imbibition processes have been investigated taking into consideration the capillary pressure and reservoir geometry. For obtaining critical curvature for drainage Mayer-Stowe-Princeton (MS-P) method was used. The critical curvature of imbibition was evaluated using Haines approximation, modified by Mason and Mellor. The model reservoir showed ~7% residual water saturation. The residual gas saturation was calculated by arbitrarily fixing the percentage of pores keeping its gas bubbles in the final stage of the process. For three situations 10%, 20%, 30% of pores trapped by CO<sub>2</sub>, the residual gas saturations was observed to be 10%, 17% and 26%, respectively .

Thus, the present study provides interesting insights into the basic aspects of the CO<sub>2</sub> sequestration, especially the mechanisms accompanying the residual (water or CO<sub>2</sub>) saturation, and the associated amounts of trapped materials. One interesting feature highlighted by the present study is the threshold effects related to the critical curvature characteristics of the reservoir. Generally speaking, the more polydisperse is the porosity of a reservoir, the more thresholds (in-or out-gassing) will be experienced through the post-injection period. As a matter of fact, this feature corresponds to pressure/volume pulses which may display negative feed-back in terms of storage security. Each time a threshold is crossed; a certain volume of CO<sub>2</sub> is trapped or pushed away, with a related brutal variation of the mechanical balance at the reservoir scale. Such very rapid events necessarily impact both the hydraulic conductivity and the local pressures, possibly contributing to affect the integrity of the reservoir (micro-fracturing). Our model reservoir is not able to simulate these consequences since it has no closed boundaries, and the liquid is free to move outside the model box during drainage at constant liquid pressure. Due to this, we do not simulate the increasing liquid pressure associated to the drainage process, and its related equilibria towards the gas pressure, these mutual changes controlling the behavior of the global bubble. As a consequence, the present strategy and calculations could be extended to complex geometries, as those defined through the packing of grains having varying and complex individual shapes. There is scope to calibrate our present model reservoir against a real system, by building a heterogeneity index (ratio between the different kinds of tetrahedral units) accounting for the pore-size distribution curves measured in the real reservoir. Further studies should open the present reasoning and considerations to practically applied calculations and predictions.

Figures

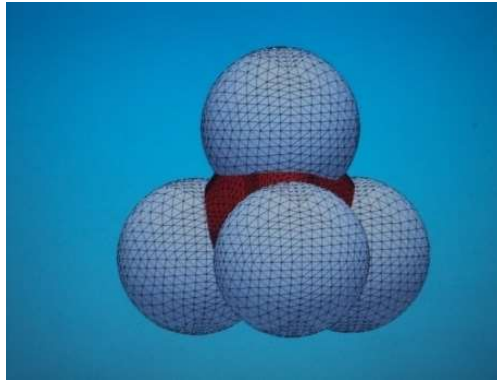


Fig. 1. Liquid bridge adhering to four spheres arranged in a tetrahedral configuration

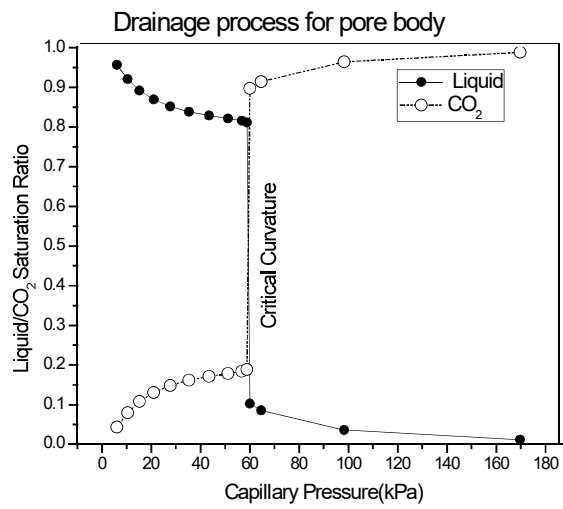


Fig.2. Variation of the liquid and CO<sub>2</sub> saturation with respect to capillary pressure

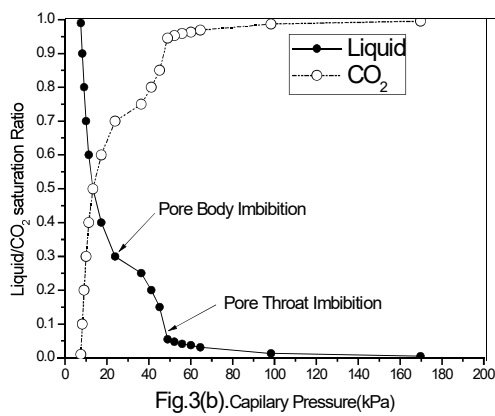
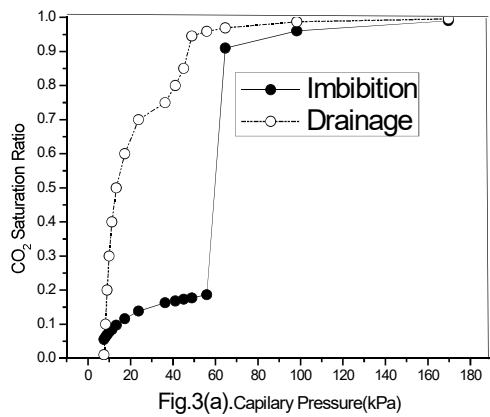


Fig. 3(a). Different steps in the imbibition process for pore body formed by four spheres arranged in tetrahedral configuration. Fig.3(b). Comparison of CO<sub>2</sub> invasion during drainage and imbibition.

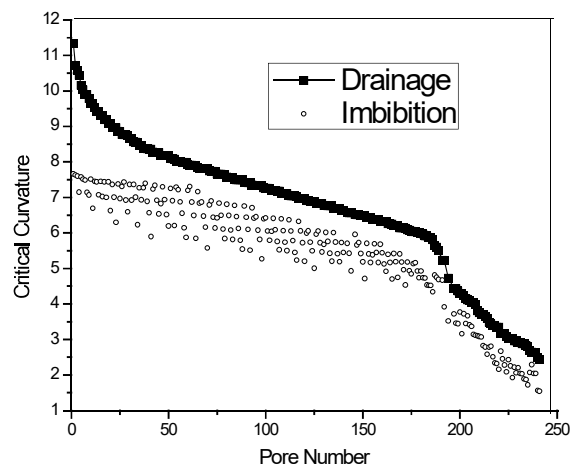


Fig. 4. Normalized critical curvatures of drainage and imbibition for the model reservoir pore bodies

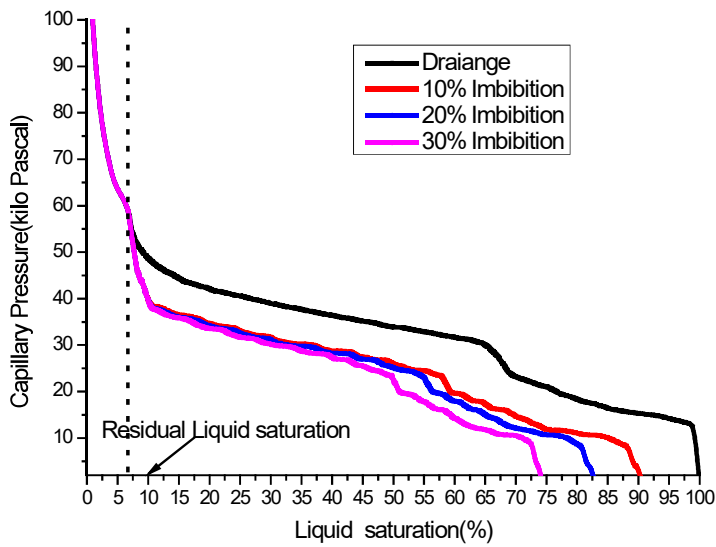


Fig. 5. Characteristic capillary pressure versus liquid saturation graph. Drainage is shown by continuous line and imbibition by broken lines. Imbibition is shown for situations with residual gas saturation filling 10%, 20%, 30% of the reservoir pores .

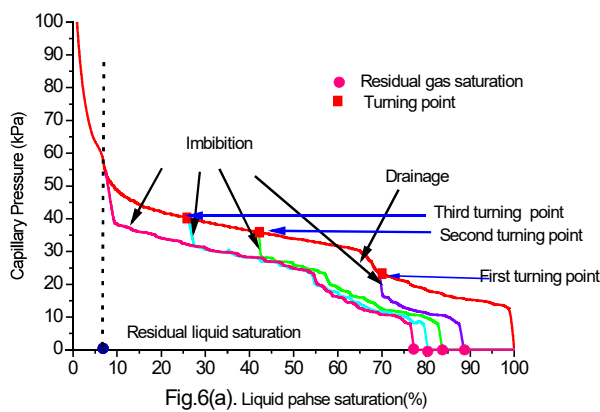


Fig.6(a). Liquid phase saturation(%)

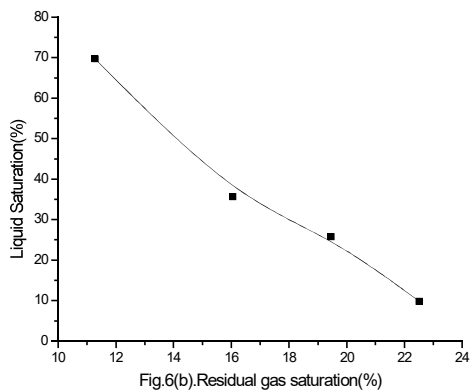


Fig.6(b).Residual gas saturation(%)

Fig. 6(a) characteristic capillary pressure curves for a model reservoir assuming 20%

pore are CO<sub>2</sub>-trapping.

Fig.6 (b) Residual gas saturation plotted as a function of liquid saturation at the turning point.

### **References**

1. Pradeep Kumar, J. ISAS., 1(3), 1, 2023.
2. Brakke A.K. Surface evolver manual. Susquehanna University Selinsgrove, PA 17870.
3. The Surface Evolver software is available on <http://www.susqu.edu/brakke/evolver>. Year 2008.
4. Haines W.B. J., Agri. Soc., 20,1930,97.
5. Mayer R.P. and Stowe R.A., J. Colloid Interf. Sci., 20,1965,93.
6. Mason G. and Marrow R.N., J. Colloid Interf. Sci., 100(2), 1984, 519.
7. Mason G. and Marrow R.N., J. Colloid Interf. Sci., 109(1), 1986, 46.
8. Mason G. and Mellor W.D. J. Colloid Interf. Sci., 176 (1995) 214.
9. Suekane T, Thanh N.H, Matsumoto T, Matsuda M, Kiyota M, Ousaka A.
10. Energy Procedia, 1, 2009, 3189.
11. Doughty C. Energy Conversion Management, 48, 2007, 1768.